Supporting Information

3D-Assembled Endohedral Nitrogen Fullerene in Metal−Organic Framework toward Spin Qubit and Quantum Sensing

Xin-Yu Hui‡, Yu-Shuang Zhang‡, Qi Xiong, Zhi-Rong Wu, Song Gao, Shen Zhou*, and Shang-Da Jiang*

Contents

SI 1: Synthesis and Characterization Methods

Synthesis of MOF-177

MOF-177 was prepared based on the literature methods[1,2]. Powder X-ray diffraction (PXRD) data of MOF-177 (Supplementary Information Figure S1) showed a close match with the theoretical result, and the cell parameters of MOF-177 determined by the single crystal X-ray diffraction (a hexagonal crystal system with cell sizes of a = 36.797 Å, b = 36.814 Å, and c = 29.796 Å at 153 K) were consistent with the previous report[2].

Synthesis of N@C_{60}@MOF-177

Add 1 ml 1000 ppm N@C_{60} solution of toluene to a sample flask containing 20 mg of MOF-177 crystals and then keep it for more than a week to ensure that N@C_{60} can fully enter the MOF-177. After that, the MOF-177 crystals changed from colorless to purple, and the color of the solution became lighter.

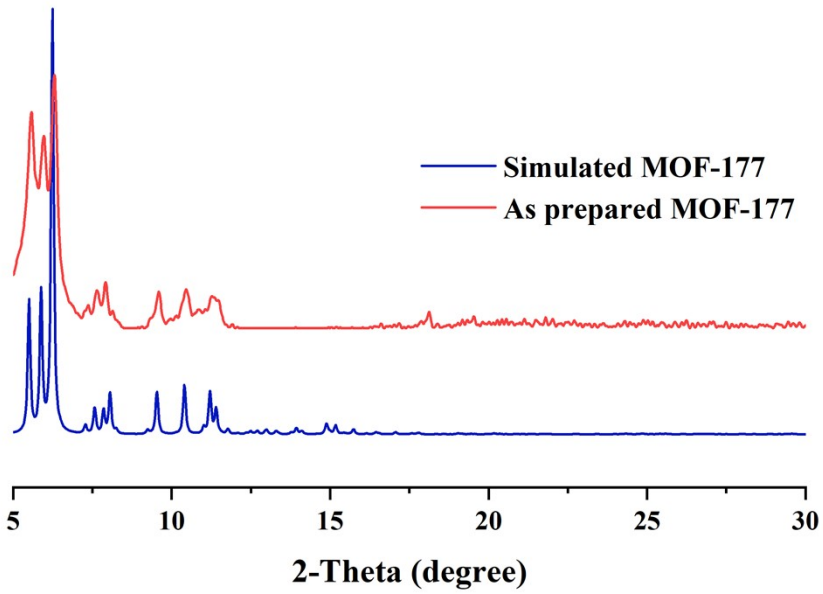

Figure S1. PXRD spectra of as-prepared **MOF-177** (red) and the simulated spectra of **MOF-177** (blue).

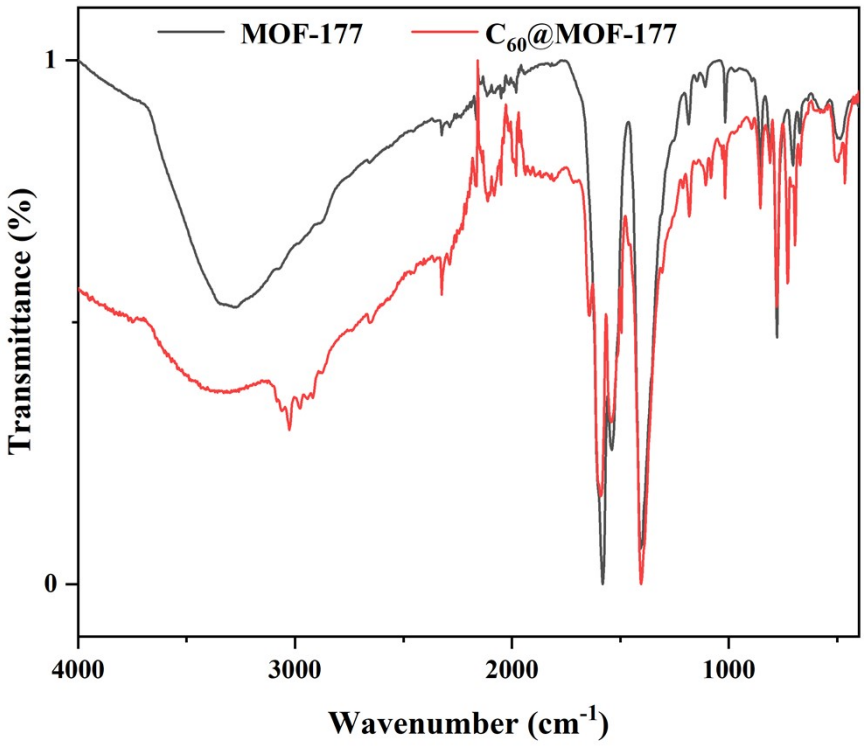

Figure S2. IR-ATR spectra of **MOF-177** powder (black) and **C_{60}@MOF-177** powder (red).

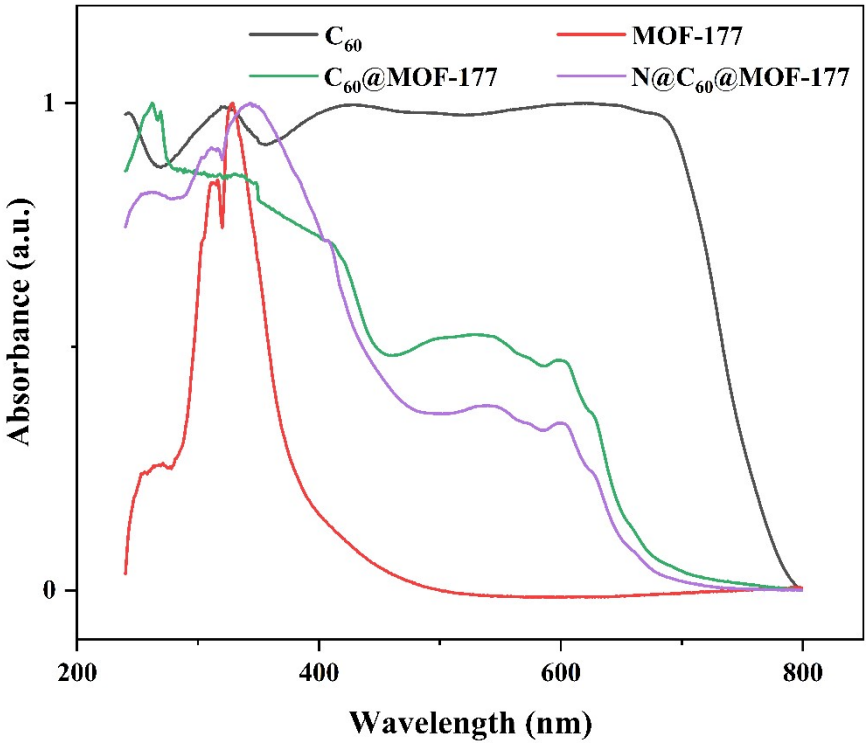

Figure S3. Solid-state Ultraviolet–visible spectra of **C_{60}** powder (black), **MOF-177** powder (red), **C_{60}@MOF-177** powder (green) and **N@C_{60}@MOF-177** powder (purple).

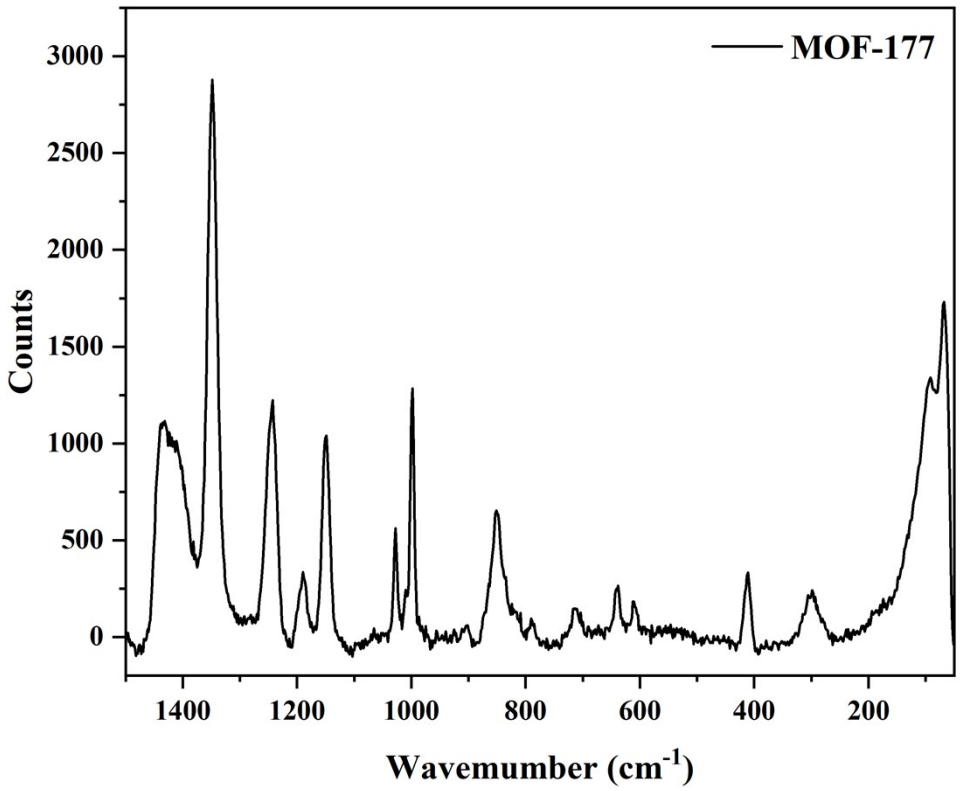

Figure S4. Raman spectra of **MOF-177** powder.

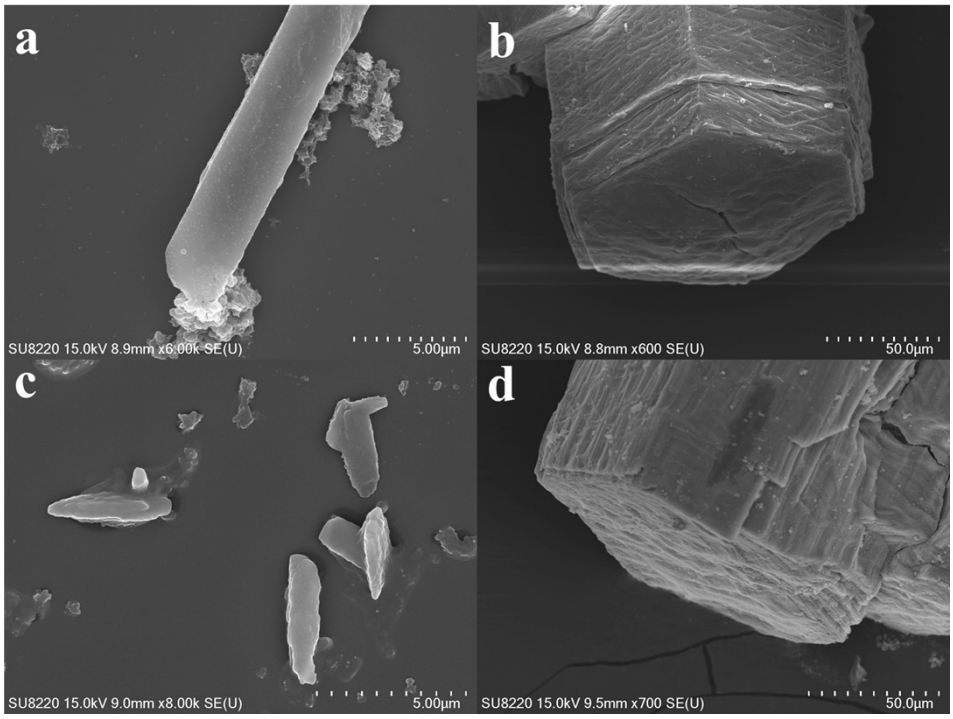

Figure S5. (a) SEM images of **MOF-177** at 5 μs scale and (b) 50 μs scale. (c) SEM images of **N@C_{60}@MOF-177** at 5 μs scale and (d) 50 μs scale.

SI 2: Variable temperature cw-EPR spectrum of $N@C_{60}$ powder

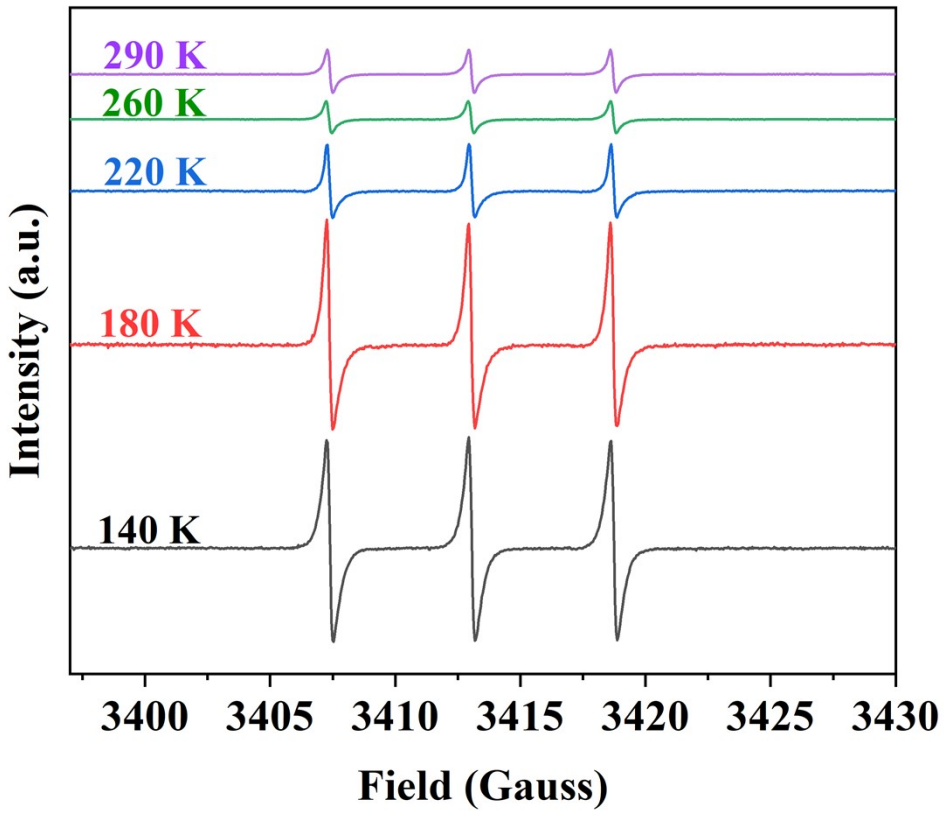

Figure S6. Variable temperature cw-EPR spectrum of $N@C_{60}$ powder.

SI 3: Simulations of EDFS spectrum of N@C_{60} powder and N@C_{60}@MOF-177 powder

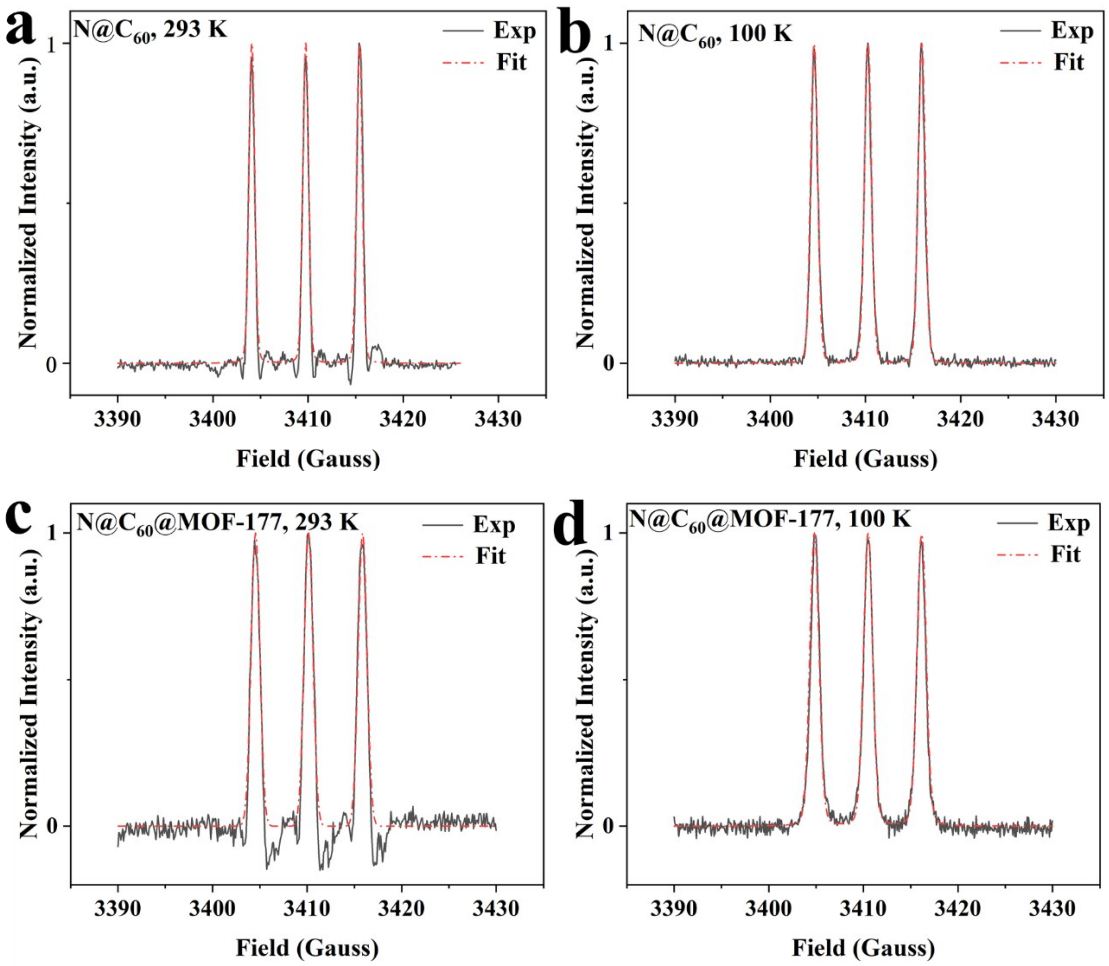

Figure S7. (a) Simulations of EDFS spectrum for **N@C_{60}** powder sample at 293 K and (b) 100 K. (c) Simulations of EDFS spectrum for **N@C_{60}@MOF-177** powder sample at 293 K and (d) 100 K.

SI 4: T_1 measurements and simulations of N@C_{60} powder and N@C_{60}@MOF-177 powder

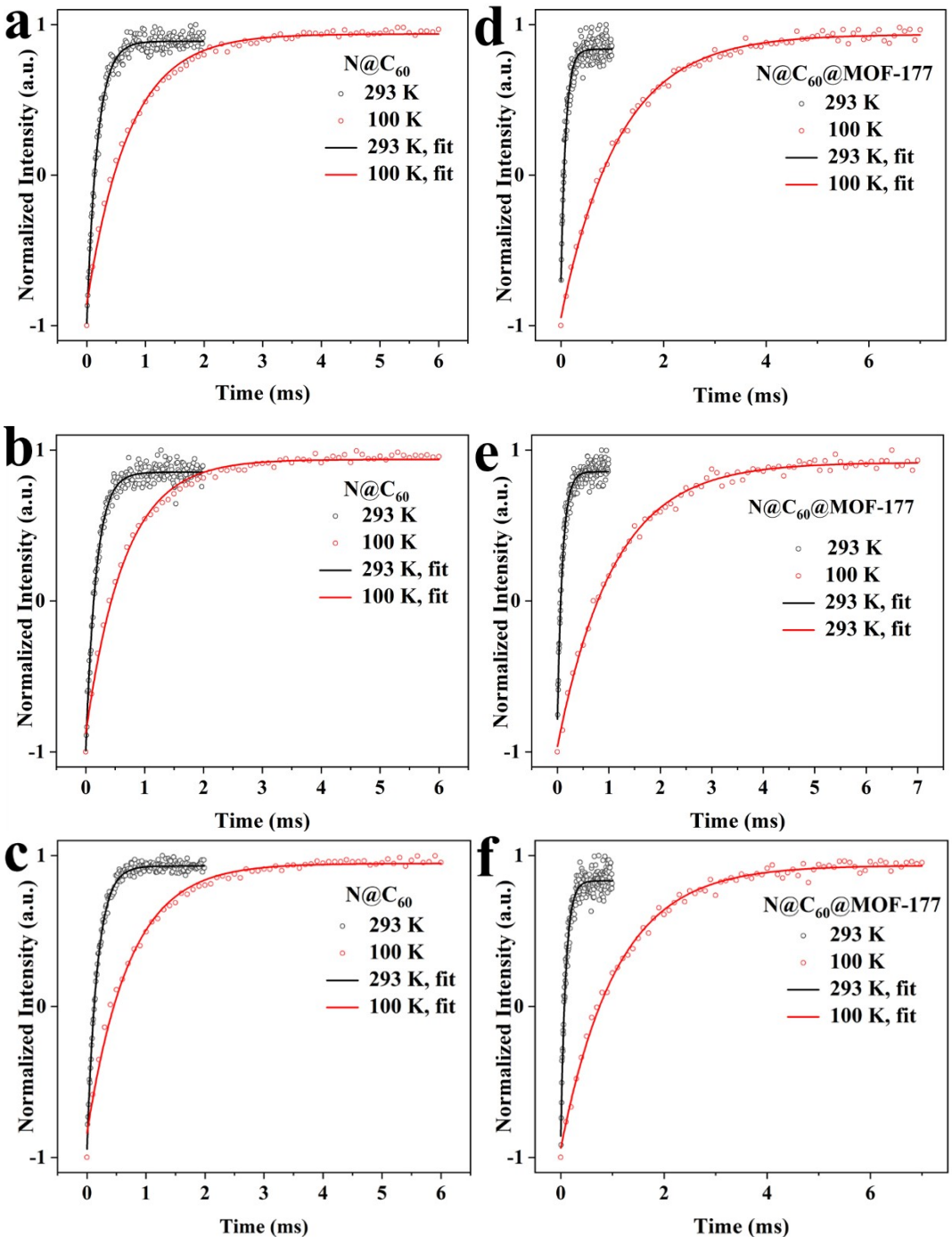

Figure S8. (a) Variable temperature T_1 data and simulations of the **N@C_{60}** powder sample at the left peak (3404.8 G) (b) the central peak (3410.6 G) and (c) the right peak (3416.1 G). (d) Variable temperature T_1 data and simulations of the **N@C_{60}@MOF-177** powder sample at the left peak (3404.8 G) (e) the central peak (3410.6 G) and (f) the right peak (3416.1 G).

All the inversion recovery data are fitted with a mono-exponential attenuation function in **Eq. S1**,

$$I(t) = I(0)\exp\left(-\frac{t}{T}\right) + C \#(Eq.S1)$$

N@C$_{60}$ powder			
T / K	T_1/ms		
	Left peak (3404.8 G)	Central peak (3410.6 G)	Right peak (3416.1 G)
293 K	0.179(1)	0.175(4)	0.173(2)
100 K	0.715(16)	0.678(13)	0.715(17)
N@C$_{60}$@MOF-177 powder			
T / K	T_1/ms		
	Left peak (3404.8 G)	Central peak (3410.6 G)	Right peak (3416.1 G)
293 K	0.093(3)	0.099(2)	0.096(3)
100 K	1.126(19)	1.101(19)	1.081(21)
10 K	-	22 (1)	-

Table S1. Variable temperature T_1 values of **N@C$_{60}$** and **N@C$_{60}$@MOF-177** powder sample. All the T_1 values were obtained at the 9.56 GHz microwave frequency with the microwave power attenuation of 18 dB.

SI 5: T_m measurements and simulations of N@C$_{60}$ powder and N@C$_{60}$@MOF-177 powder

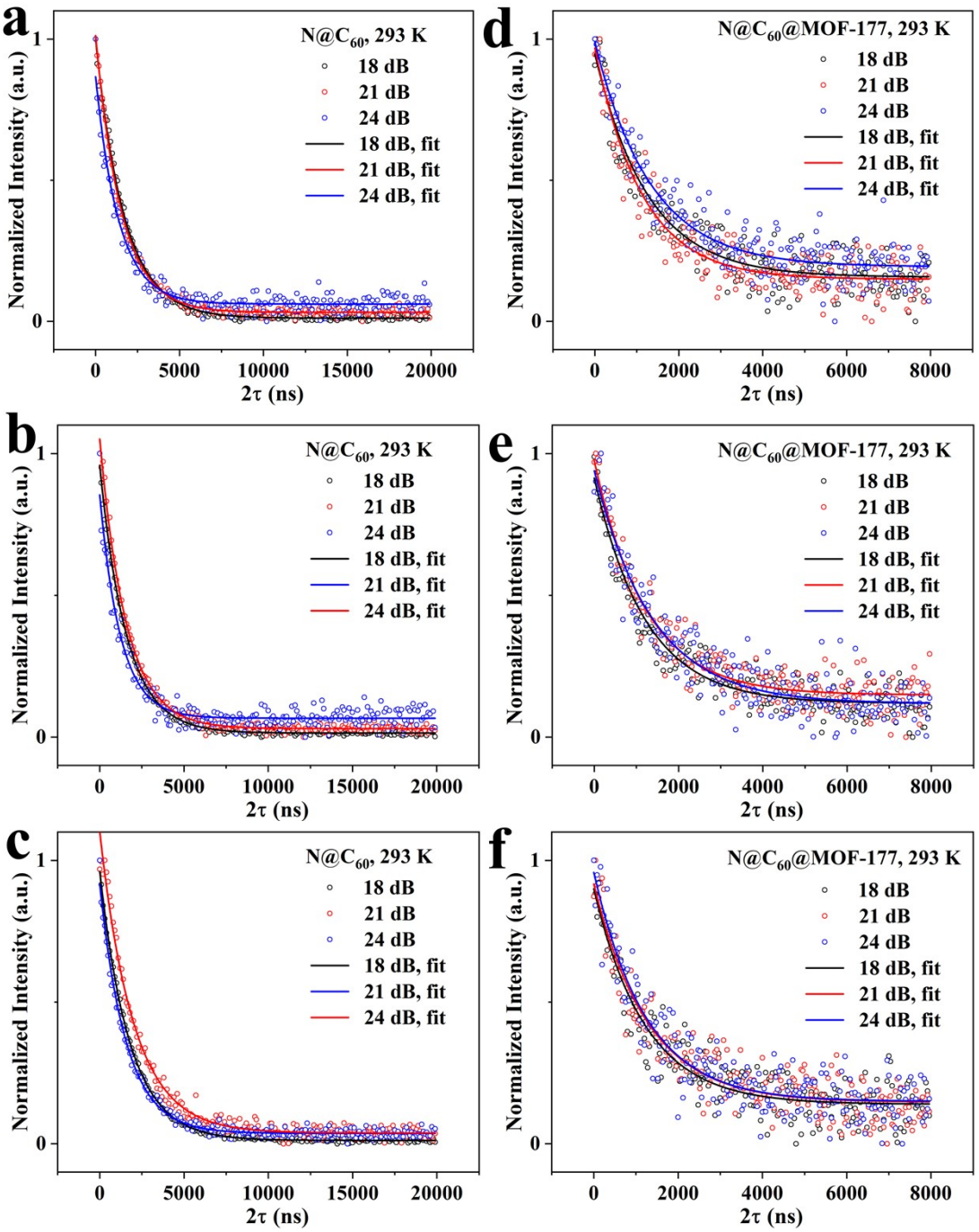

Figure S9. (a) Variable microwave power T_m data and simulations of the **N@C$_{60}$** powder sample at the left peak (3404.8 G) (b) the central peak (3410.6 G) and (c) the right peak (3416.1 G). (d) Variable microwave power T_m data and simulations of the **N@C$_{60}$@MOF-177** powder sample at the left peak (3404.8 G) (b) the central peak (3410.6 G) and (c) the right peak (3416.1 G).

All the Hahn-echo decay data are fitted with a mono-exponential attenuation function in **Eq. S1.**

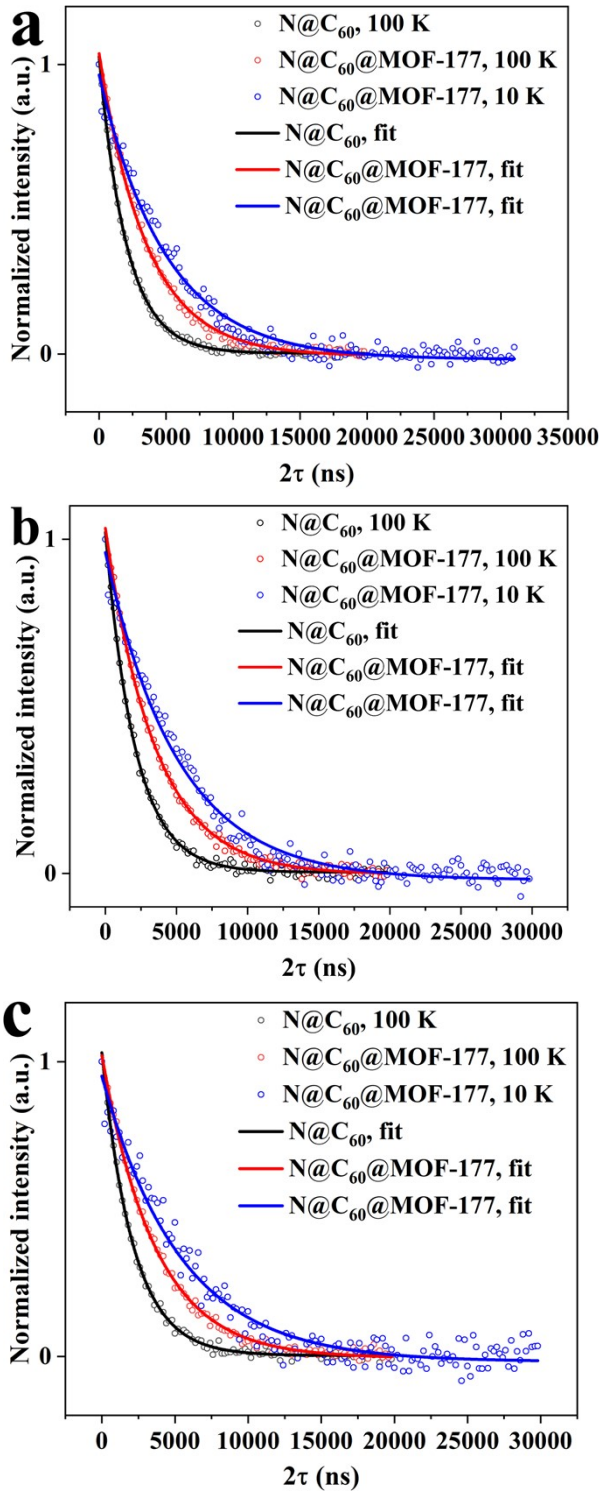

Figure S10. (a) T_m data and simulations of the **N@C$_{60}$** powder sample and **N@C$_{60}$@MOF-177** powder sample at the left peak (3404.8 G) (b) the central peak (3410.6 G) and (c) the right peak (3416.1 G) at low temperature.

N@C$_{60}$ powder			
T / K	T_m/μs		
	Left peak (3404.8 G)	Central peak (3410.6 G)	Right peak (3416.1 G)
293 K	1.700(16)[a] 1.532(15)[b] 1.383(40)[c]	1.586(11)[a] 1.569(17)[b] 1.238(41)[c]	1.773(9)[a] 1.997(32)[b] 1.568(21)[c]
100 K	2.042(17)[a]	2.092(1)[a]	2.122(23)[a]
N@C$_{60}$@MOF-177 powder			
T / K	T_m/μs		
	Left peak (3404.8 G)	Central peak (3410.6 G)	Right peak (3416.1 G)
293 K	1.263(67)[a] 1.125(59)[b] 1.334(70)[c]	1.224(53)[a] 1.216(56)[b] 1.372(76)[c]	1.214(71)[a] 1.273(75)[b] 1.237(72)[c]
100 K	3.560(47)[a]	3.507(1)[a]	3.635(46)[a]
10 K	1.97(11)[a]	5.09(12)[a]	5.36(19)[a]

Table S2. Variable temperature and microwave power T_m values of **N@C$_{60}$** powder sample and **N@C$_{60}$@MOF-177** powder sample. All the T_1 values were obtained at the 9.56 GHz microwave frequency with the microwave power attenuation of [a] 24 dB, [b] 21 dB and [c] 18 dB.

SI 6: Rabi oscillations of N@C_{60} powder and N@C_{60}@MOF-177 powder

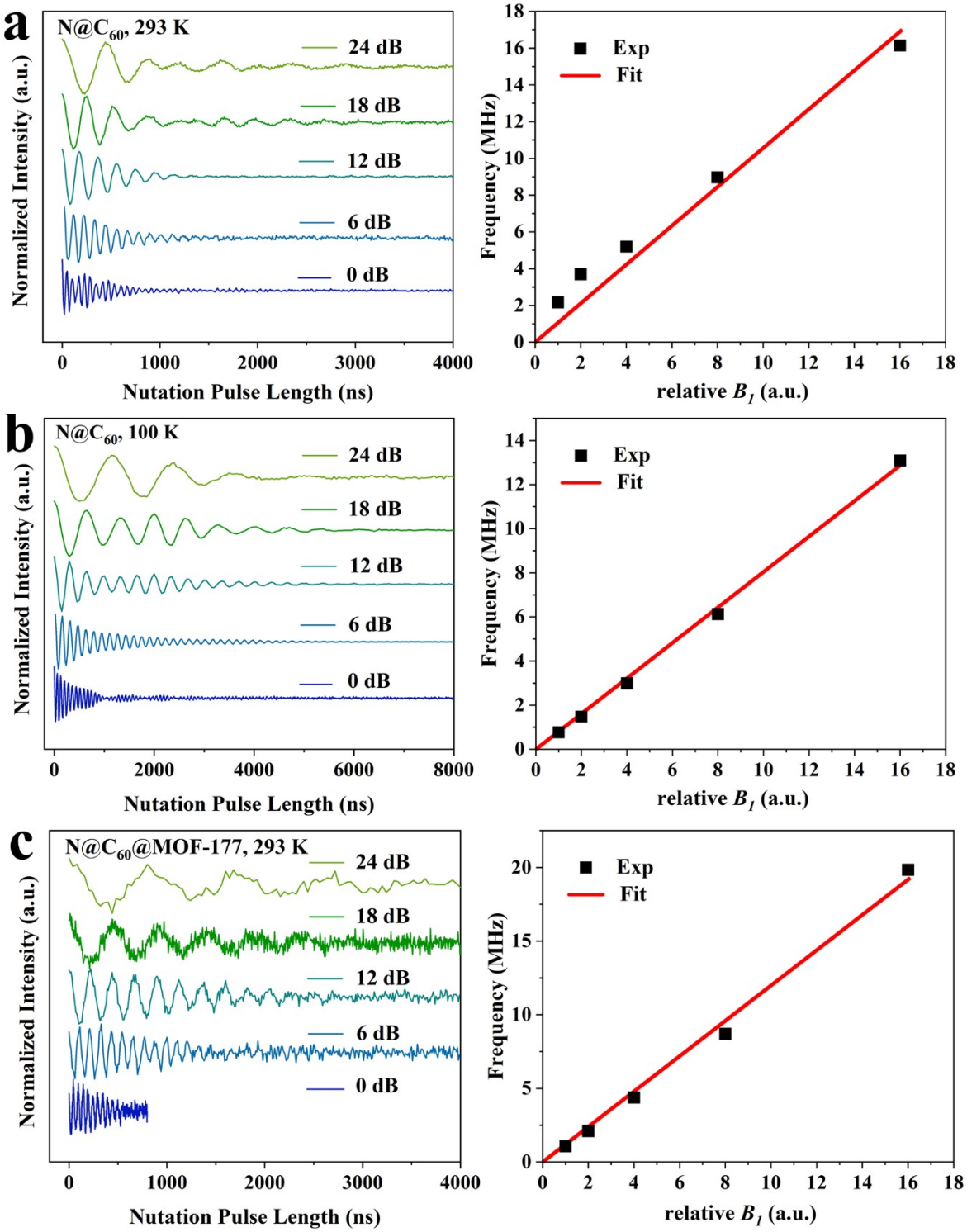

Figure S11. (a)Variable B_1 Rabi oscillation data and the linear simulations of the fast Fourier Transform (FFT) results of **N@C_{60}** powder sample at 293 K, (b)100 K and (c) **N@C_{60}@MOF-177** powder at 293 K.

SI 7: EPR measurements conditions

Both of the cw- and pulsed-EPR data were measured on X-band Chinainstru&Quantumtech (Hefei) EPR100 spectrometer with a pulse-probe cavity (9.56 GHz). The low-temperature environment was achieved by liquid helium cryostats. The signal of the pulsed-EPR experiments was collected by integrating the Hahn-echo (π/2-τ-π-τ-echo) with τ = 400 ns. The T_1 values were measured by the inversion recovery method (π-T-π/2-τ-π-τ-echo) with 2-step phase cycling. The T_m values were obtained by using the Hahn-echo sequence with 2-step phase cycling. The Rabi oscillations were obtained by nutation sequence (t_p-T-π/2-τ-π-τ-echo), where t_p is the duration time of the nutation pulse and T is longer than 5T_m. Two pulse (2p-) and three pulse (3p-) electron spin echo envelope modulation (ESEEM) experiments were carried out with the standard sequences (π/2-τ-π-τ-echo) and (π/2-τ-π/2-T-π/2-τ-echo). The π/2 and π pulse lengths in EDFS, T_1, and T_m measurements were 120 and 240 ns with 18 dB attenuation of the microwave power 450 W, respectively. In nutation experiments, the π/2 pulse lengths were adjusted to 20, 40, 80, 160 ,320 ns by 0, 6, 12, 18, and 24 dB attenuation. In 2p- and 3p-ESEEM experiments, the π/2 pulse lengths were set to 20 ns by 0 dB attenuation to collect the clear modulation signal of the ^{1}H nuclear spin.

Reference

1 Materials Design and Discovery Group, H. K. Chae, D. Y. Siberio-Pérez, J. Kim, Y. Go, M. Eddaoudi, A. J. Matzger, M. O'Keeffe and O. M. Yaghi, *Nature*, 2004, **427**, 523–527.

2 H. Meng, C. Zhao, Y. Li, M. Nie, C. Wang and T. Wang, *Nanoscale*, 2018, **10**, 3291–3298.